Maternal uterine NK cell–activating receptor KIR2DS1 enhances placentation

Shiqiu Xiong,[1] Andrew M. Sharkey,[1] Philippa R. Kennedy,[1] Lucy Gardner,[1] Lydia E. Farrell,[1] Olympe Chazara,[1] Julien Bauer,[1] Susan E. Hiby,[1] Francesco Colucci,[2] and Ashley Moffett[1]

[1]Department of Pathology and Centre for Trophoblast Research, and
[2]Department of Obstetrics and Gynaecology, University of Cambridge, Cambridge, United Kingdom.

Reduced trophoblast invasion and vascular conversion in decidua are thought to be the primary defect of common pregnancy disorders including preeclampsia and fetal growth restriction. Genetic studies suggest these conditions are linked to combinations of polymorphic killer cell Ig-like receptor (*KIR*) genes expressed by maternal decidual NK cells (dNK) and *HLA-C* genes expressed by fetal trophoblast. Inhibitory KIR2DL1 and activating KIR2DS1 both bind HLA-C2, but confer increased risk or protection from pregnancy disorders, respectively. The mechanisms underlying these genetic associations with opposing outcomes are unknown. We show that KIR2DS1 is highly expressed in dNK, stimulating strong activation of KIR2DS1$^+$ dNK. We used microarrays to identify additional responses triggered by binding of KIR2DS1 or KIR2DL1 to HLA-C2 and found different responses in dNK coexpressing KIR2DS1 with KIR2DL1 compared with dNK only expressing KIR2DL1. Activation of KIR2DS1$^+$ dNK by HLA-C2 stimulated production of soluble products including GM-CSF, detected by intracellular FACS and ELISA. We demonstrated that GM-CSF enhanced migration of primary trophoblast and JEG-3 trophoblast cells in vitro. These findings provide a molecular mechanism explaining how recognition of HLA class I molecules on fetal trophoblast by an activating KIR on maternal dNK may be beneficial for placentation.

Introduction

During early pregnancy in humans, fetal extravillous trophoblast cells (EVT) invade deeply into the mucosal lining of the uterus, the decidua, to remodel the uterine spiral arteries into high-conductance vessels (1). Reduced trophoblast invasion and vascular conversion results in poor placental perfusion, thought to be the underlying primary defect of common disorders of pregnancy, such as recurrent miscarriage, preeclampsia and fetal growth restriction, although the timing and exact clinical presentation is affected by other genetic and environmental factors (1–3). Conversely, overinvasion can result in life-threatening conditions such as placenta percreta, where trophoblast cells can rupture the uterus (4). Understanding how trophoblast invasion and arterial remodeling are regulated is therefore crucial if we are to predict which pregnancies are at risk and improve management of these disorders.

As they invade, fetal EVT encounter maternal leukocytes, approximately 70% of which are decidual NK cells (dNK) (5, 6). These are functionally and phenotypically distinct from peripheral blood NK cells (pbNK), and a growing body of evidence suggests that they play a role in regulating trophoblast invasion (7–9). EVT express a unique array of HLA class I molecules; HLA-C and nonclassical HLA-E and HLA-G, but not HLA-A or HLA-B (10–12). dNK express cognate receptors for these, such as NKG2A, LILRB1 and members of the killer cell Ig-like receptor (KIR) family (13). Because both *KIR* and their *HLA-C* ligands are highly polymorphic genes and trophoblast expresses both paternal and maternal HLA-C allotypes, each pregnancy will be characterized by different combinations of maternal *KIR* and fetal *HLA-C* genes (14–16). Inhibitory KIR that bind to HLA-C are expressed at higher frequencies in dNK than in pbNK during early pregnancy, and dNK show increased binding to HLA-C tetramers (17–19). Conversely, KIR2DL1 and KIR2DS1 Fc-fusion proteins bind directly to primary trophoblast cells, demonstrating the possibility of allogeneic recognition of fetal trophoblast by KIR on maternal dNK (14, 18).

KIR are now recognized as major regulators of NK cell function, and all individuals have HLA-C allotypes that will bind to particular KIR. Inhibitory KIR2DL1 and activating KIR2DS1 bind to allotypes of the HLA-C2 group (C2) with lysine at position 80 while inhibitory KIR2DL2/3 bind to HLA-C1 allotypes with asparagine at 80 (20, 21). There are 2 basic *KIR* haplotypes, *A* and *B*: *A* have mainly inhibitory receptors, while *B* have a variable number of additional activating receptors. We have shown that women with 2 *KIR A* haplotypes (*KIR AA* genotype) in association with a *HLA-C2* group in the fetus are at increased risk of disorders of placentation (14–16, 22). This risk is greatest if the fetal *HLA-C2* is inherited from the father and the mother lacks *HLA-C2* herself. The telomeric region of *KIR B* haplotypes (where activating *KIR2DS1* is located) provides protection from pregnancy disorders. This suggests that in *KIR AA* women, binding of inhibitory KIR2DL1 to HLA-C2 on trophoblast results in impaired trophoblast invasion. In women with a *KIR B* haplotype, activating KIR2DS1 that also binds HLA-C2, may enhance placentation by increasing invasion (14, 15).

The extracellular domain of KIR2DS1 closely resembles that of KIR2DL1 (23) but reagents are now available that allow discrimination of these inhibitory and activating receptors for HLA-C2 (24–26). When KIR2DS1$^+$ pbNK bind HLA-C2$^+$ targets, cytolysis, cytokine production, and cell proliferation are induced (24–28). Since activating KIR2DS1 may be autoreactive in *HLA-C2*$^+$ individuals, functional responses of KIR2DS1$^+$ pbNK are tuned down or educated in *C2/C2* donors compared with those who are *C1/C1* (25, 28–30). There have been no studies of expression and function of KIR2DS1 in dNK, and we therefore compared KIR2DS1 and

Authorship note: Shiqiu Xiong and Andrew M. Sharkey contributed equally to this work.

Conflict of interest: The authors have declared that no conflict of interest exists.

Citation for this article: *J Clin Invest.* 2013;123(10):4264–4272. doi:10.1172/JCI68991.

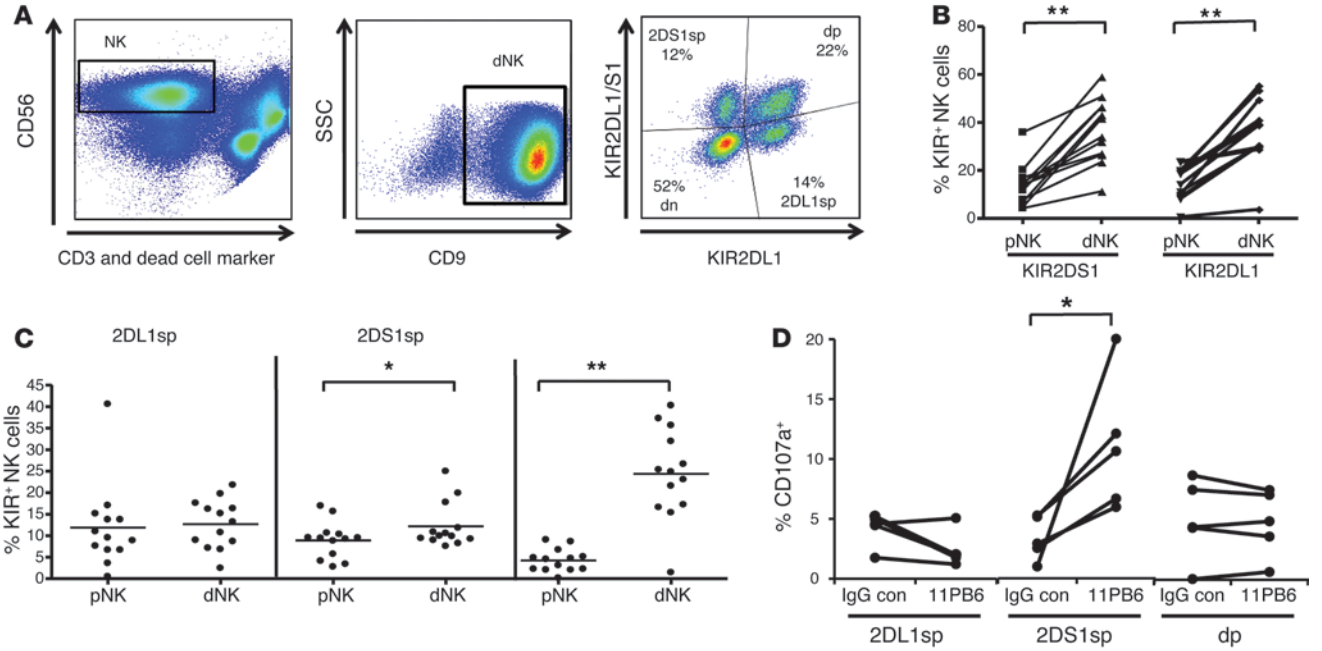

Figure 1

Frequency of KIR2DS1$^+$ and KIR2DL1$^+$ dNK is increased compared with pbNK from the same donors and KIR2DS1 is functional in dNK. (**A**) Freshly isolated leukocytes from decidua or peripheral blood were gated on live, CD56$^+$CD3$^-$ cells and examined for KIR2DS1 and KIR2DL1 expression using mAbs EB6 and 143211. dNK are shown and were also gated on CD9$^+$ cells to avoid contamination with pbNK. (**B**) Overall frequency of NK cells positive for KIR2DL1 or KIR2DS1 in paired samples from blood and decidua expressed as a percentage of total NK cells (n = 13). (**C**) Blood or dNK were classified into 4 subsets: KIR2DS1sp, dp, KIR2DL1sp, and dn as shown in **A**. The frequency of each subset as a percentage of total NK cells was determined in paired samples of fresh NK cells from blood or decidua (data for dn subset not shown, n = 13). Horizontal bars show mean for each group. (**D**) The responsiveness of the KIR2DS1sp, KIR2DL1sp, and dp dNK subsets was measured by stimulating either with control IgG (IgG con) or with mAb 11PB6, which crosslinks both KIR2DS1 and KIR2DL1. Degranulation was assessed by staining for surface CD107a or control IgG (n = 5). KIR2DL1 and KIR2DS1 subsets were gated after FACS staining, as shown in **A** and will thus express a variety of other NK receptors. Basal responses were seen in the dn subset (data not shown). *P < 0.05 and **P < 0.01, Wilcoxon paired samples test. 2DS1sp, KIR2DS1sp; 2DL1sp, KIR2DL1sp; dp, KIR2DL1$^+$KIR2DS1$^+$.

KIR2DL1 in dNK with pbNK from the same woman. We show that, like KIR2DL1, KIR2DS1 is expressed more frequently on dNK than their pbNK counterparts. KIR2DS1 is functional and triggers dNK activation. Using expression microarrays, we identified responses generated by dNK when KIR2DS1 binds HLA-C2, including secretion of cytokines such as GM-CSF, which we show enhances migration of primary trophoblast cells in vitro. These results link our genetic findings to functional responses of dNK and suggest how NK allorecognition may determine successful placentation.

Results

Expression of KIR2DL1 and KIR2DS1 by dNK. The HLA-C–specific KIR are expressed at higher frequency in dNK compared with pbNK (17–19). None of these reports distinguished between inhibitory KIR2DL1 or activating KIR2DS1, which both bind HLA-C2. Using 2 mAbs, we analyzed the frequency of KIR2DS1$^+$ and KIR2DL1$^+$ cells in matched samples of freshly isolated dNK and pbNK (Figure 1). NK cells were classified into 4 subsets: KIR2DS1$^+$KIR2DL1$^-$, KIR2DS1$^-$KIR2DL1$^+$, KIR2DS1$^+$KIR2DL1$^+$, and KIR2DS1$^-$KIR2DL1$^-$. For simplicity, these were named KIR2DS1 single positive (KIR2DS1sp), KIR2DL1sp, double positive (dp), and double negative (dn) respectively (Figure 1A).The overall frequency of KIR2DL1 expression in dNK is increased (mean 36%, range 3–55) compared with that in pbNK (mean 15%, range 1–23). KIR2DS1 is also increased in dNK (mean 36%, range 11–59) compared with blood (mean 14%, range 4–35) (Figure 1B). There is a small rise in frequency of the KIR2DS1sp subset in dNK compared with their blood counterparts, but the dp subset is significantly increased (Figure 1C). The frequencies of KIR2DL1$^+$ or KIR2DS1$^+$ dNK are unaffected by the maternal *HLA-C* genotype and are similar in women with *C1* or *C2* alleles (Supplemental Figure 1; supplemental material available online with this article; doi:10.1172/JCI68991DS1). All 4 dNK subsets shown in Figure 1A showed significantly higher staining for Ki-67 in dNK compared with their blood counterparts. This was highest in the dp subset, correlating with the increased frequency of the dp subset in dNK (Supplemental Figure 2).

KIR2DS1 on dNK is functional. To study the function of KIR2DS1, we used crosslinking with the mAb 11PB6 or a control IgG1 antibody and assessed degranulation by CD107a staining of dNK subsets expressing KIR2DL1 or KIR2DS1, gated as shown in Figure 1A. These dNK subsets will coexpress other NK receptors (NKRs). Upon crosslinking, good degranulation responses are seen in KIR2DS1sp but not in KIR2DL1sp, dp, and dn subsets, indicating KIR2DS1 is functional in dNK (Figure 1D). All subsets degranulate to the same extent using a mAb to NKp46 (Supplemental Figure 3). We then examined the function of KIR2DS1 and KIR2DL1 dNK in response to their physiological ligand HLA-C2. However, we found that other NKRs that can bind HLA-C2 directly or affect NK education (LILRB1, KIR2DL2/L3/S2, KIR3DL1, and

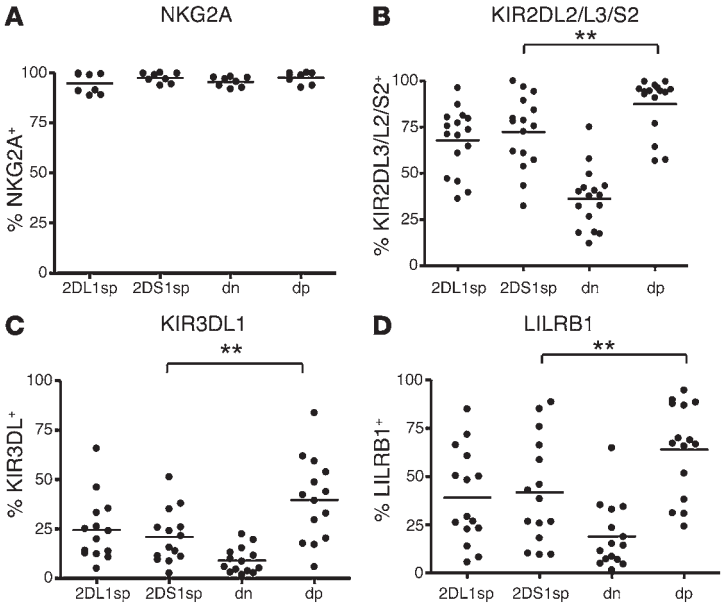

Figure 2
The phenotype of the dp cells differs from that of KIR2DL1sp and KIR2DS1sp dNK subsets. dNK were gated into 4 KIR2DL1/S1 subsets as shown in Figure 1A. The frequency of expression of selected MHC receptors was determined on each subset and then compared between the KIR2DS1sp and dp subsets. Horizontal bars show mean for each group. For NKG2A, $n = 8$; KIR2DL3/L2/S2, $n = 16$; KIR3DL1, $n = 14$; LILRB1, $n = 15$. $^{**}P < 0.01$, Mann-Whitney test.

KIR2DS4) are not expressed equally on the KIR2DS1sp and dp dNK subpopulations (Figure 2, B–D, and Supplemental Figure 4). Therefore, to examine the functional responses of the KIR2DL1/S1 subsets to HLA-C2 in the absence of such confounding effects, dNK expressing these other NKRs were gated out from the analysis, except where specifically stated. Significant degranulation of KIR2DS1sp cells was seen in response to 721.221 cells transfected with HLA-Cw*0602 (221-C2) that was abolished by coincubation with the anti–HLA class I–blocking mAb 6A4 (Figure 3, A and B). As with activation by crosslinking, no significant degranulation was seen in KIR2DL1sp or dp subsets, indicating that inhibition by KIR2DL1 overrides activation of KIR2DS1 by HLA-C2 when they are coexpressed. Coexpression of other NKRs that recognize HLA class I resulted in decreased responses of KIR2DS1sp dNK to 221-C2, but these responses were still significantly higher than in the dp subset (Figure 3C). KIR2DS1sp dNK that are also NKR$^+$ make up approximately 11% of the total dNK population (Supplemental Figure 5A). Individual NKRs differ in their effect on the degranulation response of KIR2DS1sp dNK with 221-C2 target cells, with coexpression of LILRB1 having the least effect and KIR2DL1 the most (Supplemental Figure 5B). Activation of KIR2DS1sp dNK in response to 221-C2 targets is higher in dNK from *C1/C1* homozygous individuals compared with those with at least 1 copy of *HLA-C2* (*C2/X*) (Figure 3D).

Because NK cells are sensitive to levels of HLA class I expression, we compared how KIR2DS1sp pbNK and dNK from the same donor responded to 221-C2 targets with increasing levels of surface expression of the same HLA-C2 allele (Cw*0602). KIR2DS1sp dNK showed lower maximal responses than their pbNK counterparts, but in both, the level of response was dependent on the target HLA-C expression level (Figure 3, E and F, and Supplemental Figure 6). dNK achieved maximal activation at lower HLA-C2 levels on 221-C2 target cells, suggesting they are more sensitive than pbNK to low levels of KIR2DS1 ligand.

Transcriptional responses of KIR2DS1$^+$ or KIR2DL1$^+$ dNK triggered by HLA-C2 ligand. Ligation of activating receptors on NK cells triggers a variety of responses, including cytokine secretion and expression of molecules involved in cell-cell adhesion (31). We used gene expression microarrays to investigate the changes in RNA transcript levels in the 4 KIR2DS1 or KIR2DL1 dNK subsets from a single donor that were triggered in response to coculture with either 721.221-parent (221-parent) or 221-C2 cells. Cluster analysis showed that each subset has a distinctive mRNA expression profile (Figure 4A). Only 45 transcripts differ by 2.5-fold in the KIR2DL1sp subset, while in the KIR2DS1sp subset, 378 transcripts differ by at least 2.5-fold in expression level and 289 transcripts differ in the dp subset (Supplemental Table 1). Remarkably, only 24 transcripts were altered in common between the KIR2DS1sp and the dp subset even though they both expressed KIR2DS1. The small degree of overlap suggests that each subset has its own unique response to HLA-C2. We were particularly interested in factors that might be directly responsible for paracrine modulation of EVT migration and focused on altered transcripts encoding cytokines or cell surface receptors/adhesion molecules (Figure 4C). Transcripts for 4 secreted proteins were upregulated in KIR2DS1sp dNK more than 2.5-fold: IFN-γ, CSF2 (GM-CSF), and chemokines XCL2 and CCL3L3. IFN-γ was not specifically upregulated by KIR2DS1, since it was also increased in the other subsets (Supplemental Table 1).

We focused on GM-CSF to demonstrate how activation of KIR2DS1 might enhance placentation. Intracellular staining for GM-CSF confirmed that KIR2DS1sp dNK (without expression of other NKR) specifically upregulate GM-CSF production after coculture with 221-C2 cells compared with the KIR2DL1sp and dp subsets (Figure 5A and Supplemental Figure 7A). KIR2DS1$^+$ dNK (with expression of other NKRs but not KIR2DL1) also showed increased intracellular staining for GM-CSF, although this response was lower than for KIR2DS1sp NKR$^-$ cells. This suggests that KIR2DS1 triggering by HLA-C2 upregulates GM-CSF even in cells that coexpress inhibitory NKRs that can bind HLA-C2. These results were confirmed using crosslinking with mAb EB6, which binds both KIR2DS1 and KIR2DL1 in samples of bulk dNK. GM-CSF secretion was detected by ELISA in culture supernatants and was significantly increased in KIR2DS1$^+$ but not KIR2DS1$^-$ donors after cross-linking (Figure 5B). Despite the fact that KIR2DS1$^+$

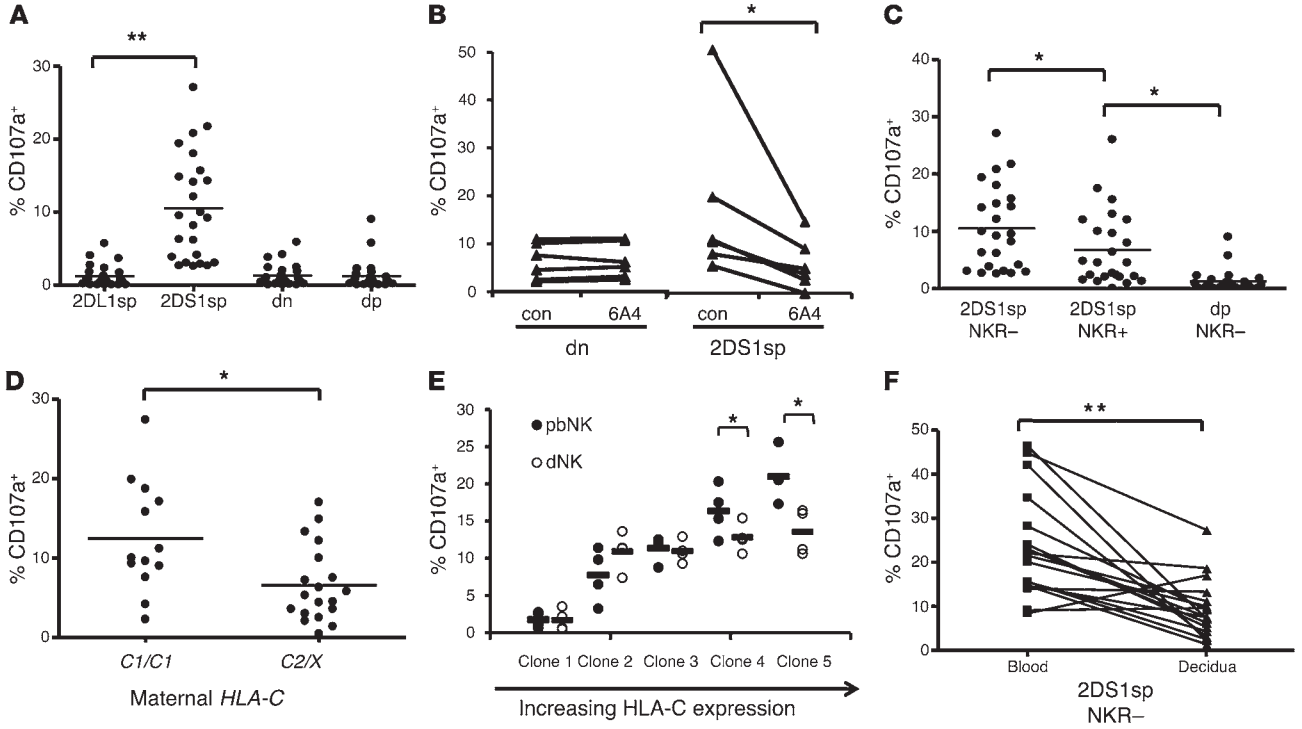

Figure 3

KIR2DS1sp dNK respond to HLA-C2+ target cells. dNK expressing other NKRs (LILRB1, KIR2DL2/L3/S2, KIR3DL1, and KIR2DS4) were gated out from the analysis, except where stated. (**A**) CD107a staining was measured in the 4 dNK subsets after incubation with 221-C2 target cells ($n = 25$). Horizontal bars indicate mean for each group. (**B**) Analysis similar to that in **A**, but performed in the presence of the HLA class I blocking mAb 6A4 or isotype control (con) ($n = 6$). (**C**) Effect of other NKRs on KIR2DS1 responses to 221-C2 targets. After culture with 221-C2 targets, KIR2DS1+ dNK were gated into 3 subsets: KIR2DS1sp with no other NKRs expressed (2DS1sp NKR+), KIR2DS1sp that do coexpress other NKRs apart from KIR2DL1 (2DS1sp NKR+) and dp cells without other NKRs (dp NKR–). Frequency of CD107a+ dNK was compared between the 3 different subsets ($n = 24$). (**D**) Effect of donor's *HLA-C* genotype on KIR2DS1 response. Degranulation of KIR2DS1sp NKR– subset in response to culture with 221-C2 targets was compared between donors who had at least one *HLA-C2* allele (*C2/X*, $n = 19$) and donors homozygous for *HLA-C1* (*C1/C1*, $n = 13$). (**E**) Degranulation of the KIR2DS1sp NKR– subset from matched pbNK and dNK was measured after coculture with 4 different 221-C2 clones expressing different surface levels of the HLA-C2 allele Cw*0602 (Supplemental Figure 6). Clone 1 is 221-parent. Horizontal bars indicate means for 4 separate donors. (**F**) Degranulation of the KIR2DS1sp NKR– subset in response to the same clone of 221-C2 target cells by pbNK and dNK from the same donor ($n = 18$). *$P < 0.05$ and **$P < 0.01$, Mann-Whitney test (**A**, **C**, and **D**). *$P < 0.05$ and **$P < 0.01$, Wilcoxon paired samples test (**B** and **F**). *$P < 0.05$, Student's paired *t*-test (**E**).

cells that do not coexpress KIR2DL1 represent approximately 13% of total dNK (Supplemental Figure 5A), activation of KIR2DS1 does result in significant GM-CSF secretion.

GM-CSF produced by dNK after activation of KIR2DS1 stimulates trophoblast migration in vitro. We then investigated the function of GM-CSF in enabling normal placentation because our genetic data suggests that binding of KIR2DS1 on dNK to trophoblast HLA-C2 is beneficial when there is a *HLA-C2* group in the fetus. First, we localized expression of GM-CSF receptor α (GM-CSFRα) in vivo by immunohistochemistry. There was intense expression of GM-CSFRα by interstitial EVT in decidua at sites densely infiltrated by maternal dNK, where dNK can be seen closely associated with EVT (Figure 6, A–E). GM-CSFRα expression was confirmed by flow cytometry using primary trophoblast cells (Figure 6F) and the choriocarcinoma cell line JEG-3 (data not shown). Supernatants of dNK in which KIR2DS1 had been activated by crosslinking contained increased levels of GM-CSF as shown in Figure 5B. These supernatants stimulated JEG-3 migration through fibronectin-coated Transwells and the effect was significantly reduced by addition of neutralizing GM-CSF antibody, compared with supernatant with isotype control mAb added (Figure 6G). Recombinant GM-CSF also increased the migration of primary trophoblast cells through Transwells and enhanced the motility of JEG-3 cells in a scratch assay (Figure 6H and Supplemental Figure 8). Thus, KIR2DS1+ dNK produced GM-CSF following activation, and this enhanced the migration of primary trophoblast and choriocarcinoma cells in vitro.

Discussion

The response of maternal uterine NK cells to allogeneic fetal trophoblast at the site of placentation is analogous to the situation during HSC transplantation (HSCT) when donor cells confront allogeneic recipient cells (32–34). Women with *KIR AA* genotypes who lack *HLA-C2* but have a *HLA-C2*+ fetus are most at risk of pregnancy disorders such as preeclampsia. *KIR2DS1* is located in the telomeric region of *KIR B* haplotypes and is associated with protection from pregnancy disorders when the fetus is *HLA-C2*+ (14, 15, 22) Similarly, patients with myeloid leukemia who receive grafts from donors with *KIR B* haplotypes that contain *KIR2DS1* show improved survival (35). This effect depends on the *HLA-C1* or *HLA-C2* status of the donor and is stronger if the donor lacks *HLA-C2* but it is present in the recipient. We therefore set out to determine

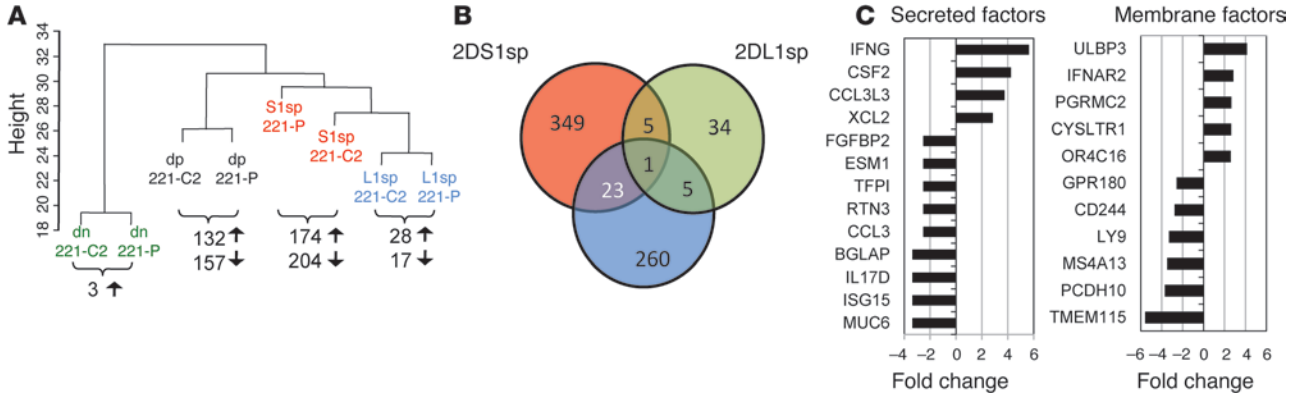

Figure 4
Transcriptional responses of KIR2DS1sp and KIR2DL1sp dNK subsets to 221-C2 cells. Four KIR2DL1/S1 subsets from a single donor were purified by FACS to identify transcripts that altered after coculture with 221-C2 compared with 221-parent (221-P) target cells. (**A**) Organization and length of the dendrogram branches reflect the degree of similarity between samples. Numbers beneath each pair show the number of transcripts that change in hybridization intensity by at least 2.5-fold. Direction of change (up or down) is indicated. (**B**) Venn diagram showing comparison of transcripts that differ by more than 2.5-fold in each subset. (**C**) RNA transcripts encoding secreted factors or surface membrane receptors that differ by at least 2.5-fold in the KIR2DS1sp subset. Transcripts were classified according to Gene Ontology annotations.

how our genetic findings in pregnancy translate into some dNK function beneficial for placentation during early pregnancy.

Initially, we studied the expression of KIR2DS1 in dNK. Overall frequencies of both KIR2DL1 and KIR2DS1 are dramatically increased in dNK compared with pbNK from the same donor. The number of dNK that coexpress both receptors was somewhat larger than predicted by the product rule (36). How the selective increase of KIRs in dNK specific for HLA-C occurs in the decidual microenvironment is unknown, but it is a response to pregnancy, since it is not seen in nonpregnant endometrium (13). The dp cells do proliferate more than the KIR2DS1sp and KIRDL1sp subsets, which may partially explain their prominence in the decidua. IL-15 is transpresented by stromal cells during decidualization and can induce dNK proliferation, maturation, and acquisition of KIR, but not this skewing toward KIR2D specific for HLA-C (13, 37–40). TGF-β can affect the phenotype of dNK and is abundant in decidua (39–41). Changes in MHC class I molecules expressed by stromal cells can also modulate the receptor repertoire of NK cells in vitro or after HSCT (42–44). Although expression of HLA-C on uterine stromal cells increases during decidualization, with the modest numbers studied here, we found no association between maternal *HLA-C1* or *HLA-C2* and KIR2DL1 or KIR2DS1 frequencies in dNK, as previously shown by others in pbNK (25, 45). Sample numbers did not permit us to determine whether fetal *HLA-C1* or *HLA-C2* affects KIR2DL1/S1 frequencies independently of maternal *HLA-C*. Decidual stroma and dNK are in intimate contact but the exact factors responsible for expansion of this dp remain unclear. Nonetheless, the outcome is that whenever a paternal *HLA-C2* is expressed by trophoblast, there will be large numbers of dNK potentially able to respond to this nonself *HLA-C*. The finding that allogeneic mouse matings differing only in paternal MHC produce heavier fetuses than syngeneic matings strongly supports the idea that recognition of paternal MHC by maternal immune cells is a generalized mechanism to regulate placental development (46).

Triggering of dNK with mAb to KIR2DL1/S1 or with HLA-C2$^+$ targets results in selective degranulation and cytokine secretion by the KIR2DS1sp cells, but all subsets respond to the same extent when triggered by mAb to NKp46. In addition, a mAb (6A4) known to block binding of KIR2DS1 to HLA-C2$^+$ targets inhib-

Figure 5
Activation of KIR2DS1 by HLA-C2 or crosslinking results in GM-CSF production. (**A**) Intracellular staining for GM-CSF in KIR2DL1/S1 subsets after coculture of dNK with 221-C2 targets. Frequencies of GM-CSF$^+$ dNK were compared between different subsets: KIR2DS1sp with no other NKRs expressed (2DS1sp NKR$^-$), KIR2DS1sp that do coexpress other NKRs apart from KIR2DL1 (2DS1sp NKR$^+$), and dp cells without other NKRs (dp NKR$^-$). GM-CSF staining in KIR2DL1sp and dn subsets was similar to that in the dp subset (data not shown). $^{**}P < 0.01$, Mann-Whitney test. (**B**) Increased GM-CSF secretion in supernatants of dNK from KIR2DS1$^+$ donors after antibody crosslinking. Total dNK from KIR2DS1$^+$ or KIR2DS1-ve donors were crosslinked for 12 hours with EB6 or IgG control and GM-CSF measured in supernatants by ELISA. $^*P < 0.05$, Wilcoxon signed rank test.

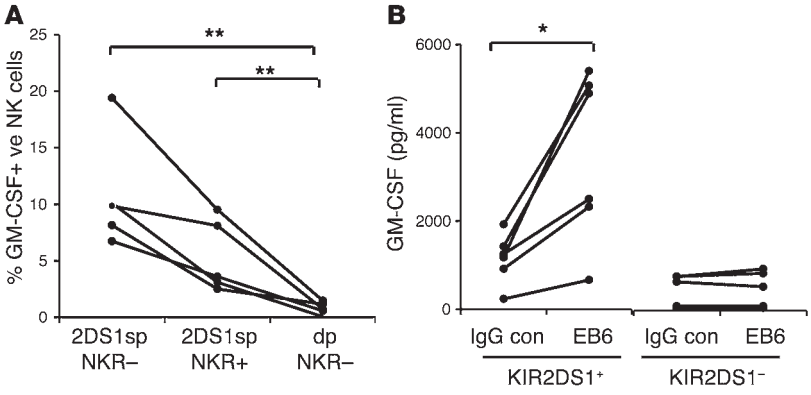

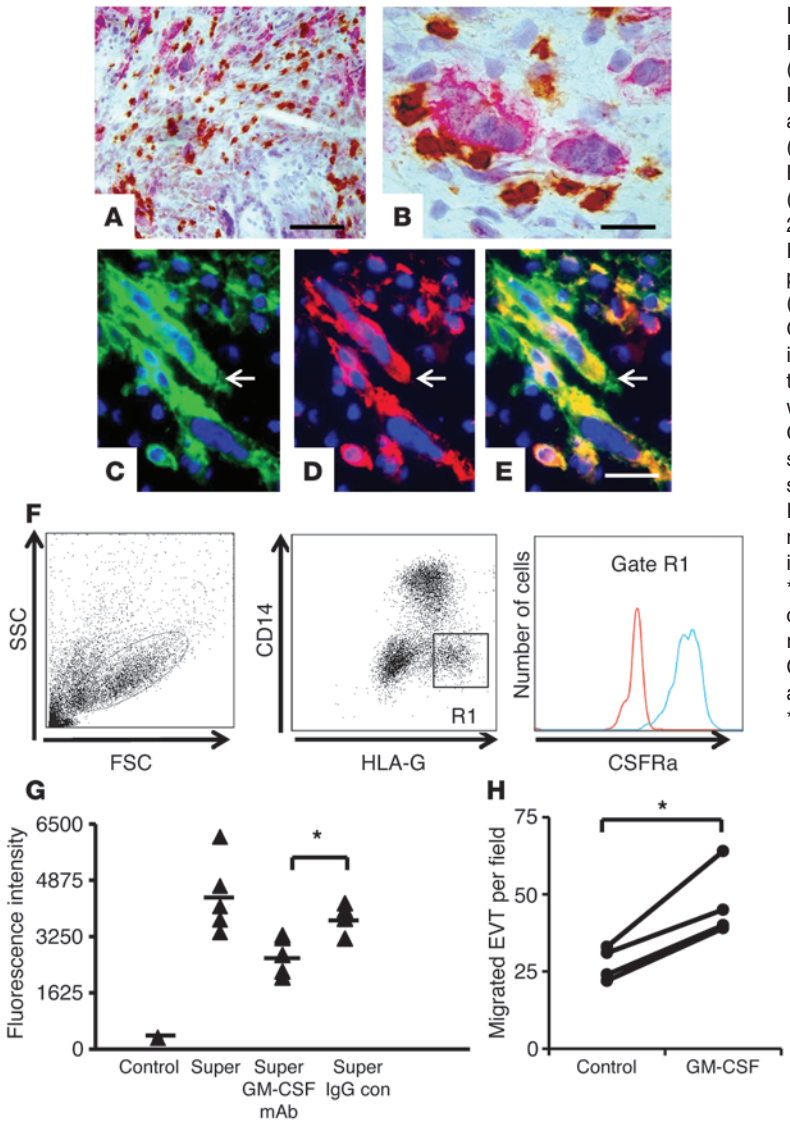

Figure 6
Effect of GM-CSF on trophoblast migration. (**A**) Immunohistochemistry of human implantation site. HLA-G$^+$ EVT (red) and CD56$^+$ dNK (brown). (**B**) The close association of dNK with EVT is obvious at higher power. (**C**–**E**) Immunofluorescence staining of serial section to **A**. HLA-G$^+$ EVT (green, arrow in **C**) coexpress GM-CSFRα (red, **D**) as seen in the overlay in **E**. Scale bars: 250 μm (**A**); 25 μm (**B**–**E**). (**F**) Expression of GM-CSFRα on primary EVTs (stained for HLA-G in gate R1 after gating out CD14$^+$ placental macrophages). Histogram shows isotype control (red line) and GM-CSFRα staining (blue line) of the HLA-G$^+$ EVT in R1. (**G**) JEG-3 cells show increased migration in a Transwell assay in response to supernatant conditioned by dNK from KIR2DS1$^+$ donors after crosslinking with EB6 (super). Addition of neutralizing antibody against GM-CSF to the supernatant (super + GM-CSF mAb) significantly reduced JEG-3 migration compared with supernatant plus isotype control mAb (super + IgG con). Results are presented as the calcein dye fluorescence measured in the lower chamber 48 hours after seeding. Horizontal bars show mean for each group (n = 5). *P < 0.05, Student's paired t test. (**H**) Primary trophoblast cells show increased migration in a Transwell assay in response to 10 ng/ml GM-CSF added to the lower chamber. Control wells had no added GM-CSF. Results are presented as the number of EVT counted in the sampled fields (n = 4). *P < 0.01, Student's t test.

its KIR2DS1sp activation (47). The *HLA-C1* or *HLA-C2* status of the mother is also important as KIR2DS1sp dNK from *C1/C1* donors respond better to HLA-C2$^+$ targets than those from *C2/C1* heterozygotes. This contrasts with pbNK, where tuning down of KIR2DS1 responses to HLA-C2 was observed only in *HLA-C2* homozygotes (25, 26, 29, 30). The rheostat model of NK education proposes that NK cell function is "tuned" by interactions between inhibitory and activating receptors on the cell and their ligands during NK development, and quantity of MHC also affects NK cell responsiveness (48, 49). Indeed, we show that dNK appear to be more sensitive to lower levels of HLA-C, and this may explain why we found evidence of dNK tuning via KIR2DS1 even in C2/C1 heterozygotes. Since these mature dNK proliferate in situ, tuning presumably takes place or is maintained within the decidua. These functional findings correlate well with our genetic studies of pregnancy disorders in which the presence/absence of *HLA-C2* in the mother as well as the baby influences the outcome (14).

CD107a is a convenient measure of NK cell activation in response to HLA-C2, but cytokine production is more physiologically relevant to pregnancy (7). To avoid nonphysiological responses due to culture with high levels of IL-2 or IL-15, we used primary dNK exposed overnight to a low dose of IL-15, which maintains good viability with minimal activation (50, 51). Under these conditions, IFN-γ is not a useful readout, as the levels produced and number of dNK responding is low (31, 52). Therefore, we used microarrays to identify the mRNA responses of KIR2DL1/S1 subsets following coculture with either 221-C2 or 221-parent cells. In KIR2DS1sp cells, which degranulate in response to HLA-C2, nearly 400 transcripts change, but in KIR2DL1sp cells, which do not degranulate, the transcriptional responses are subdued. In dp cells, KIR2DL1 overrides any degranulation stimulated by KIR2DS1, as it does in pbNK, but other aspects of the response are robust. This suggests divergence of the pathways regulating degranulation and the transcriptional responses mediated by KIR2DS1 in dp cells. Surprisingly, there was very little overlap in the transcriptional responses of the KIR2DS1sp and the dp subsets. Although we excluded confounding factors such as expression of other NKRs that might be responsible for different levels of

dNK education in the initial dNK preparation for the microarrays, we found that each KIR2DL1/S1 subset had a complex and unique response to HLA-C2. The molecular basis for this is not clear, but the responses generated by KIR2DS1 were thus context dependent, and this receptor may trigger completely different transcriptional responses in KIR2DS1sp and dp subsets. This aspect of the responses of different dNK subsets to HLA-C2 may well apply to other activating and inhibitory receptor combinations when they are coexpressed in other NK subsets. The microarray analysis was performed on the 4 KIR2DL1 and KIR2DS1 subsets from a single donor and must therefore be treated with caution. However, the fact that the GM-CSF response of KIR2DS1sp cells identified in this way was validated at the protein level in multiple other donors increases confidence in this approach.

dNK do not normally kill trophoblast cells unless activated by IL-2, but this cytokine is not found in the decidua. Instead, their function is probably to produce cytokines, enzymes, and other products that may regulate trophoblast invasion (7, 31, 53–55). Given the protective effect of KIR2DS1 in our genetic studies of preeclampsia, we therefore sought proteins induced after stimulation of KIR2DS1$^+$ dNK by HLA-C2$^+$ targets. Of those we identified, GM-CSF was studied in detail to demonstrate that dNK products induced by ligation of maternal KIR by fetal HLA-C can regulate placentation. Secretion of GM-CSF is specifically upregulated in KIR2DS1sp but not dp dNK after coculture with HLA-C2$^+$ target cells. Although the KIR2DS1sp subset accounts for a minority of the total dNK compartment, activation of KIR2DS1 results in increased GM-CSF secretion into supernatants of bulk dNK preparations. The GM-CSFRα is strongly expressed by the EVT in decidua that are in close contact with dNK. In vitro, GM-CSF enhances invasion by primary trophoblast as well as JEG-3 choriocarcinoma cells. Studies in GM-CSF–deficient mice support the idea that placental development and fetal growth are impaired in the absence of maternal GM-CSF, but the mechanism of this effect is unknown (56). The mechanisms regulating trophoblast migration and transformation of the spiral arteries are complex, and other dNK products induced by activation of KIR2DS1, including chemokines and cytokines, will also be important. Indeed, we only saw partial reduction of trophoblast migration with a GM-CSF–blocking antibody. Our hypothesis was that activation of KIR2DS1 by a HLA-C2$^+$ fetus enhances trophoblast invasion and vascular transformation of spiral arteries. This process is frequently defective in pregnancies affected by disorders such as preeclampsia and FGR, as shown by uterine artery Dopplers and anatomical studies of the placental bed (3). We propose that, in a KIR2DS1$^+$ woman with a HLA-C2$^+$ fetus, the dNK activation that ensues allows trophoblast to invade even more deeply into the decidua. In contrast, women with only KIR2DL1 and a HLA-C2 fetus are at risk of pregnancy disorders where EVT may not effectively transform the more distal myometrial segments of the spiral arteries. Exactly how the process is regulated in vivo in the deeper portions of the decidua and myometrium is not known, but one possibility is that, as well as encouraging migration, KIR2DS1 activation also prevents EVT differentiation to static giant cells. Until more reliable human trophoblast cell lines become widely available, it will be difficult to investigate this further.

In conclusion, our observations suggest how women with KIR2DS1 and a HLA-C2$^+$ fetus may have better trophoblast invasion and spiral artery remodeling than women with *KIR AA* genotypes who are at higher risk of preeclampsia (57). Activation of KIR2DS1 on dNK by HLA-C triggers responses that enhance trophoblast migration and also change the responses of dNK that coexpress the "risky" inhibitory receptor KIR2DL1. Our study thus provides what we believe is the first important link between dNK function and our genetic studies showing that particular combinations of maternal *KIR* and fetal *HLA-C* genotypes are associated with different pregnancy outcomes.

Methods

Primary tissue. Decidua were obtained from donors undergoing elective termination between 7 and 12 weeks of pregnancy. Primary trophoblast cells and decidual leukocytes (DL) were isolated by enzymatic digestion of placental or decidual tissue as described previously (58). Trophoblast cells were cultured overnight in Ham's F12, antibiotics, and 20% FCS on fibronectin before analysis by FACS with HLA-G–specific antibody (clone MEM-G/9; AbD Serotec). Decidual samples were analyzed by FACS after staining with anti-CD56, anti-CD3, and anti-CD9 to evaluate peripheral blood contamination (8, 13). DL preparations were typically composed of more than 50% dNK. For functional assays, DL preparations were cultured overnight in RPMI 1640 medium, antibiotics, 10% FCS. and 2.5 ng/ml IL-15. This low dose of IL-15 maintains dNK viability without significant activation (50). PBMCs were isolated from the same donor at the same week of gestation using Lymphoprep (Axis-Shield) and stained or cultured in same conditions as for DL.

Genotyping of KIR and HLA-C. *KIR* and *HLA-C* were typed from genomic DNA by PCR for their presence or absence as described previously (14, 15). *KIR* genes typed were *3DL1*, *3DS1*, *2DL1*, *2DL2*, *2DL3*, *2DL5*, *2DS1*, *2DS2*, *2DS3*, *2DS4*, *2DS5*, and *2DP1*. Typing for *HLA-C* was performed using a similar approach, which allowed all known *HLA-C* group *HLA-C1* alleles to be distinguished from *HLA-C2* alleles.

Phenotyping NK cells and trophoblast by flow cytometry. 10^6 fresh cells from blood or decidua were washed with PBS, resuspended in 100 μl FACS buffer (PBS + 1% FCS + 0.1% sodium azide), and incubated with 5 μg/ml human γ-globulins (Sigma-Aldrich) for 15 minutes to block nonspecific binding. To determine the frequency of KIR2DL1 and KIR2DS1, cells were stained with 10 μl KIR2DL1-FITC mAb (clone 143211; R&D Systems) for 15 minutes at room temperature. Then 5 μl KIR2DL1/S1-APC mAb (clone EB6; Beckman Coulter) was added together with antibodies against other surface markers for 20 minutes at 4°C. Other antibodies used were as follows: KIR2DL2/L3/S2-PE (clone GL183), LILRB1-PE (clone HP-F1), NKG2A-PE (clone Z199), and KIR2DS4 (clone FES172) (Beckman Coulter); KIR3DL1-PE (clone DX9; BD Biosciences), CD56–brilliant violet (clone HCD56; Biolegend), CD3-APC-Cy7 (clone UCHT1; BioLegend), and CD9-PerCP Cy5.5 (M-L13, BD Biosciences – Pharmingen). Further details of antibodies used in multicolor flow cytometry are given in Supplemental Table 2. Dead cells were excluded with near IR fixable live/dead cell dye (Invitrogen). Cells were washed with FACS buffer twice and fixed in 2% paraformaldehyde. Samples were run on LSR Fortessa FACS analyzer (BD Biosciences) and data analyzed using FlowJo 8.0. Freshly isolated primary trophoblast cells and the JEG-3 choriocarcinoma cell line were analyzed by flow cytometry as previously described (12). Briefly, cells were stained with directly conjugated mAb to identify leukocyte or trophoblast cell populations using MEM-G/9-FITC to HLA-G (AbD Serotec) and CD14-PE (clone HCD14; BioLegend).

Functional assays. DL preparations (>50% dNK) with less than 5% pbNK contamination (CD56$^+$CD9$^-$) were used in functional assays. For KIR crosslinking followed by flow cytometry, 96-well plates (Costar EIA) were coated with crosslinking antibody against KIR2DL1/S1 (clone 11PB6; Miltenyi Biotec) or NKP46 (clone 195314; R&D Systems) in 50 mM HEPES buffer for 4 hours at concentrations between 0 and 10 μg/ml. Optimal antibody con-

centration (2.5 μg/ml) was determined by titration. Matched isotype mAbs were used as controls. 2×10^5 dNK per well were incubated for 5 hours. 6 μg/ml Golgi-Stop (BD Biosciences) and Brefeldin (Sigma-Aldrich) were added for the last 4 hours of the incubation. The degranulation response was assessed by staining with anti-CD107a–PerCP Cy5.5 (clone H4A3; BioLegend) after first staining dNK subsets as described above. EB6 was used for KIR2DL1/S1 crosslinking to assess GM-CSF secretion by ELISA with no Golgi-Stop or Brefeldin added. GM-CSF secretion was quantified using the Duoset ELISA (R&D Systems).

NK cells were also stimulated by incubation with 721.221 HLA-null parent cells (221-parent), or with 721.221 cells transfected either with the group 2 HLA-C allele Cw*0602 (221-C2) or 721.221 cells expressing Cw*0102 (221-C1). Medium alone or phorbol-12-myristate-13-acetate (PMA) (20 ng/ml) and ionomycin (1 μg/ml) together were used as negative and positive controls. The effector/target (E/T) ratio was 5:1. To obtain 221-C2 clones with different HLA-C2 surface expression intensity, bulk 221-C2 cells were diluted in 96-well plates at 1 cell per well. Individual clones were stained with mAb W6/32 to identify those with different HLA-C expression. Readouts of NK activation were as follows: CD107a or the cytokines IFN-γ (clone 4S.B3 Biolegend) or GM-CSF (clone BVD2-21C11; BD Bioscience). Cells were first stained for surface markers to identify KIR2DL1 and KIR2DS1 NK subsets, then fixed, permeabilized, and stained for intracellular cytokines with PerCP Cy5.5 mAbs using intracellular staining buffers (BioLegend).

Expression profiling by microarray. Total dNK were purified by negative selection using MACS beads (Miltenyi Biotec) after overnight culture in RPMI with 10% FCS and 2.5 ng/ml IL-15. The purified dNK were then cocultured in a 1:1 ratio with either 221-parent or 221-C2 cells for 12 hours in the same medium. KIR2DL1/S1 subsets of dNK ($CD56^+CD9^+CD3^-$) were sorted using a DakoCytomation MoFlo cytometer and Summit software after gating out cells expressing KIR3DL1, KIR2DL3/L2/S2, LILRB1, and KIR2DS4. Total RNA was isolated from each subset using RNEasy (QIAGEN). cDNA was synthesized using 50 ng of total RNA and biotinylated using the Pico WTA system and Encore module (Nugen). Biotinylated cDNA was hybridized to Human HT-12 V4 BeadArrays (Illumina). Background corrected and summarized expression scores for each microarray probe set were converted to $\log_2$ expression units and normalized by Quantile normalization implemented in the lumi package for Bioconductor (59). Microarray data are available from the ArrayExpress microarray data repository (E-MTAB-1784).

Chemotaxis and cell motility assays. Migration assays using the choriocarcinoma line JEG-3, were performed in 24-well plates using Transwell inserts with 12-μm pores (PIXPO1250; Millipore) coated with 1 μg/ml fibronectin (BD Biosciences). JEG-3 cells were grown in RPMI, 10% FCS. and seeded at 2×10^4 cells per insert, with or without GM-CSF added to the medium in the lower part of the chamber. After 48 hours. the number of JEG-3 cells that had migrated into the lower chamber was quantified by the addition of calcein AM (4 μg/ml) to the lower chamber for 1 hour as described by the manufacturer (Biotium) and total fluorescence measured using a Synergy HT plate reader (Biotek). When using primary trophoblast cells, the cells were allowed to migrate for 48 hours and the cells on the upper side of the membrane were removed with a cotton bud so that only the migrated cells on the underside were quantified by staining with anti–cytokeratin-7 antibody (clone MNF116; Dako) as described previously (60). This method ensures only migrating trophoblast cells were counted, since primary cultures are not completely pure. The number of trophoblast cells that had migrated was quantified by counting cytokeratin$^+$ cells at 800 random points on the membrane using Visiopharm software. The effect of GM-CSF on trophoblast motility was assessed using a "scratch"' wound-healing assay. 3.5×10^4 JEG-3 were seeded in a culture-insert dish overnight (product 81176; Ibidi) and the insert removed to create a defined "wound" of 500 μm in width at the start of the experiment. The medium was changed (with or without 10 ng/ml GM-CSF added) and cells photographed at indicated time points to monitor cell motility.

Immunohistology. 5 μm cryostat sections of the first-trimester human implantation site were fixed in cold acetone, rehydrated with PBS, and blocked with PBS/1% BSA/2% goat serum before staining for 1 hour with mAb for GM-CSFRα (clone 4H1; BioLegend) diluted 1/50. Slides were washed in PBS, then bound antibody visualized with goat-anti-mouse IgG1–Alexa Fluor 568 (Invitrogen). Free anti-mouse sites were blocked with mouse IgG (1 μg/ml) before staining with anti–HLA-G-FITC for 1 hour (clone MEM-G/9; AbD Serotec). Slides were rinsed in PBS and mounted with Vectashield containing DAPI (Vector Laboratories) and photographed on a Zeiss Axiophot fluorescent microscope.

Statistics. The Wilcoxon signed rank test was used to compare 2 groups of paired data, and the Mann-Whitney test was used for comparison of groups of nonpaired data. Student's *t* test (2 tailed) was employed for analyzing normally distributed data obtained from cell lines in vitro. A nonparametric Friedman test with Dunn multiple comparison post test was used to test for differences in between multiple KIR2DS1sp subsets with different NKRs. $P < 0.05$ was considered statistically significant.

Study approval. The Cambridge Research Ethics Committee approved this study (04/Q0108/23 and 08/H0305/40). Informed written consent was obtained from all donors.

Acknowledgments

The authors thank Diane Moore and all the clinical staff and donors at Addenbooke's Hospital, Cambridge, without whom this study would not have been possible. We also thank Nigel Miller and Rachel Walker for invaluable assistance with FACS sorting and the staff of the Cambridge Genomic Services microarray facility. This work was supported by funding from the Wellcome Trust (090108/Z/09/Z, 085992/Z/08/Z), and the British Heart Foundation (PG/09/077/27964). P.R. Kennedy was in receipt of a Wellcome Trust PhD studentship. The authors also thank the Centre for Trophoblast Research for generous support.

Received for publication January 24, 2013, and accepted in revised form July 19, 2013.

Address correspondence to: Ashley Moffett, Department of Pathology and Centre for Trophoblast Research, University of Cambridge, Tennis Court Road, Cambridge CB2 1QP, United Kingdom. Phone: 44.1223.333729; Fax: 44.1223.333346; E-mail: am485@cam.ac.uk.

1. Moffett A, Loke C. Immunology of placentation in eutherian mammals. *Nat Rev Immunol*. 2006; 6(8):584–594.
2. Brosens I, Pijnenborg R, Vercruysse L, Romero R. The "Great Obstetrical Syndromes" are associated with disorders of deep placentation. *Am J Obstet Gynecol*. 2011;204(3):193–201.
3. Roberts JM, Escudero C. The placenta in preeclampsia. *Pregnancy Hypertens*. 2012;2(2):72–83.
4. Jauniaux E, Jurkovic D. Placenta accreta: pathogenesis of a 20th century iatrogenic uterine disease. *Placenta*. 2012;33(4):244–251.
5. King A, Balendran N, Wooding P, Carter NP, Loke YW. CD3- leukocytes present in the human uterus during early placentation: phenotypic and morphologic characterization of the CD56++ population. *Dev Immunol*. 1991;1(3):169–190.
6. Bulmer JN, Morrison L, Longfellow M, Ritson A, Pace D. Granulated lymphocytes in human endometrium: histochemical and immunohistochemical studies. *Hum Reprod*. 1991; 6(6):791–798.
7. Hanna J, et al. Decidual NK cells regulate key developmental processes at the human fetal-maternal interface. *Nat Med*. 2006;12(9):1065–1074.
8. Koopman LA, et al. Human decidual natural killer cells are a unique NK cell subset with immunomodu-

latory potential. *J Exp Med*. 2003;198(8):1201–1212.
9. Moffett-King A. Natural killer cells and pregnancy. *Nat Rev Immunol*. 2002;2(9):656–663.
10. King A, et al. Surface expression of HLA-C antigen by human extravillous trophoblast. *Placenta*. 2000; 21(4):376–387.
11. Kovats S, Main EK, Librach C, Stubblebine M, Fisher SJ, DeMars R. A class I antigen, HLA-G, expressed in human trophoblasts. *Science*. 1990; 248(4952):220–223.
12. Apps R, Murphy SP, Fernando R, Gardner L, Ahad T, Moffett A. Human leucocyte antigen (HLA) expression of primary trophoblast cells and placental cell lines, determined using single antigen beads to characterize allotype specificities of anti-HLA antibodies. *Immunology*. 2009;127(1):26–39.
13. Male V, Sharkey A, Masters L, Kennedy PR, Farrell LE, Moffett A. The effect of pregnancy on the uterine NK cell KIR repertoire. *Eur J Immunol*. 2011; 41(10):3017–3027.
14. Hiby SE, et al. Maternal activating KIRs protect against human reproductive failure mediated by fetal HLA-C2. *J Clin Invest*. 2010;120(11):4102–4110.
15. Hiby SE, et al. Combinations of maternal KIR and fetal HLA-C genes influence the risk of preeclampsia and reproductive success. *J Exp Med*. 2004; 200(8):957–965.
16. Parham P, Guethlein LA. Pregnancy immunogenetics: NK cell education in the womb? *J Clin Invest*. 2010;120(11):3801–3804.
17. Verma S, King A, Loke YW. Expression of killer cell inhibitory receptors on human uterine natural killer cells. *Eur J Immunol*. 1997;27(4):979–983.
18. Sharkey AM, et al. Killer Ig-like receptor expression in uterine NK cells is biased toward recognition of HLA-C and alters with gestational age. *J Immunol*. 2008;181(1):39–46.
19. Marlin R, et al. Dynamic shift from CD85j/ILT-2 to NKG2D NK receptor expression pattern on human decidual NK during the first trimester of pregnancy. *PLoS One*. 2012;7(1):e30017.
20. Chazara O, Xiong S, Moffett A. Maternal KIR and fetal HLA-C: a fine balance. *J Leukoc Biol*. 2011; 90(4):703–716.
21. Parham P, Norman PJ, Abi-Rached L, Hilton HG, Guethlein LA. Review: Immunogenetics of human placentation. *Placenta*. 2012;33(suppl):S71–S80.
22. Hiby SE, Regan L, Lo W, Farrell L, Carrington M, Moffett A. Association of maternal killer-cell immunoglobulin-like receptors and parental HLA-C genotypes with recurrent miscarriage. *Hum Reprod*. 2008;23(4):972–976.
23. Biassoni R, et al. Role of amino acid position 70 in the binding affinity of p50.1 and p58.1 receptors for HLA-Cw4 molecules. *Eur J Immunol*. 1997; 27(12):3095–3099.
24. Sivori S, Carlomagno S, Falco M, Romeo E, Moretta L, Moretta A. Natural killer cells expressing the KIR2DS1-activating receptor efficiently kill T-cell blasts and dendritic cells: implications in haploidentical HSCT. *Blood*. 2011;117(16):4284–4292.
25. Fauriat C, Ivarsson MA, Ljunggren HG, Malmberg KJ, Michaelsson J. Education of human natural killer cells by activating killer cell immunoglobulin-like receptors. *Blood*. 2010;115(6):1166–1174.
26. Cognet C, et al. Expression of the HLA-C2-specific activating killer-cell Ig-like receptor KIR2DS1 on NK and T cells. *Clin Immunol*. 2010;135(1):26–32.
27. Rose MJ, Brooks AG, Stewart LA, Nguyen TH, Schwarer AP. Killer Ig-like receptor ligand mismatch directs NK cell expansion in vitro. *J Immunol*. 2009; 183(7):4502–4508.
28. Foley B, De Santis D, Lathbury L, Christiansen F, Witt C. KIR2DS1-mediated activation overrides NKG2A-mediated inhibition in HLA-C C2-negative individuals. *Int Immunol*. 2008;20(4):555–563.
29. Chewning JH, Gudme CN, Hsu KC, Selvakumar A, Dupont B. KIR2DS1-positive NK cells mediate alloresponse against the C2 HLA-KIR ligand group in vitro. *J Immunol*. 2007;179(2):854–868.
30. Pittari G, et al. NK cell tolerance of self-specific activating receptor KIR2DS1 in individuals with cognate HLA-C2 ligand. *J Immunol*. 2013;190(9):4650–4660.
31. Vacca P, et al. Regulatory role of NKp44, NKp46, DNAM-1 and NKG2D receptors in the interaction between NK cells and trophoblast cells. Evidence for divergent functional profiles of decidual versus peripheral NK cells. *Int Immunol*. 2008; 20(11):1395–1405.
32. Cooley S, et al. Donor selection for natural killer cell receptor genes leads to superior survival after unrelated transplantation for acute myelogenous leukemia. *Blood*. 2010;116(14):2411–2419.
33. Marcenaro E, Carlomagno S, Pesce S, Della Chiesa M, Moretta A, Sivori S. Role of alloreactive KIR2DS1(+) NK cells in haploidentical hematopoietic stem cell transplantation. *J Leukoc Biol*. 2011; 90(4):661–667.
34. Miller JS, Blazar BR. Control of acute myeloid leukemia relapse--dance between KIRs and HLA. *N Engl J Med*. 2012;367(9):866–868.
35. Venstrom JM, et al. HLA-C-dependent prevention of leukemia relapse by donor activating KIR2DS1. *N Engl J Med*. 2012;367(9):805–816.
36. Andersson S, Fauriat C, Malmberg JA, Ljunggren HG, Malmberg KJ. KIR acquisition probabilities are independent of self-HLA class I ligands and increase with cellular KIR expression. *Blood*. 2009; 114(1):95–104.
37. Male V, Hughes T, McClory S, Colucci F, Caligiuri MA, Moffett A. Immature NK cells, capable of producing IL-22, are present in human uterine mucosa. *J Immunol*. 2010;185(7):3913–3918.
38. Kitaya K, Yasuda J, Yagi I, Tada Y, Fushiki S, Honjo H. IL-15 expression at human endometrium and decidua. *Biol Reprod*. 2000;63(3):683–687.
39. Keskin DB, et al. TGFbeta promotes conversion of CD16+ peripheral blood NK cells into CD16- NK cells with similarities to decidual NK cells. *Proc Natl Acad Sci U S A*. 2007;104(9):3378–3383.
40. Vacca P, et al. CD34+ hematopoietic precursors are present in human decidua and differentiate into natural killer cells upon interaction with stromal cells. *Proc Natl Acad Sci U S A*. 2011;108(6):2402–2407.
41. Stoikos CJ, Harrison CA, Salamonsen LA, Dimitriadis E. A distinct cohort of the TGFbeta superfamily members expressed in human endometrium regulate decidualization. *Hum Reprod*. 2008;23(6):1447–1456.
42. Joncker NT, Shifrin N, Delebecque F, Raulet DH. Mature natural killer cells reset their responsiveness when exposed to an altered MHC environment. *J Exp Med*. 2010;207(10):2065–2072.
43. Roth C, Carlyle JR, Takizawa H, Raulet DH. Clonal acquisition of inhibitory Ly49 receptors on developing NK cells is successively restricted and regulated by stromal class I MHC. *Immunity*. 2000; 13(1):143–153.
44. Roth C, Rothlin C, Riou S, Raulet DH, Lemke G. Stromal-cell regulation of natural killer cell differentiation. *J Mol Med (Berl)*. 2007;85(10):1047–1056.
45. Schonberg K, Sribar M, Enczmann J, Fischer JC, Uhrberg M. Analyses of HLA-C-specific KIR repertoires in donors with group A and B haplotypes suggest a ligand-instructed model of NK cell receptor acquisition. *Blood*. 2011;117(1):98–107.
46. Madeja Z, et al. Paternal MHC expression on mouse trophoblast affects uterine vascularization and fetal growth. *Proc Natl Acad Sci U S A*. 2011; 108(10):4012–4017.
47. Stewart CA, et al. Recognition of peptide-MHC class I complexes by activating killer immunoglobulin-like receptors. *Proc Natl Acad Sci U S A*. 2005; 102(37):13224–13229.
48. Brodin P, Lakshmikanth T, Johansson S, Karre K, Hoglund P. The strength of inhibitory input during education quantitatively tunes the functional responsiveness of individual natural killer cells. *Blood*. 2009;113(11):2434–2441.
49. Almeida CR, Ashkenazi A, Shahaf G, Kaplan D, Davis DM, Mehr R. Human NK cells differ more in their KIR2DL1-dependent thresholds for HLA-Cw6-mediated inhibition than in their maximal killing capacity. *PLoS One*. 2011;6(9):e24927.
50. Apps R, et al. Ex vivo functional responses to HLA-G differ between blood and decidual NK cells. *Mol Hum Reprod*. 2011;17(9):577–586.
51. Verma S, Hiby SE, Loke YW, King A. Human decidual natural killer cells express the receptor for and respond to the cytokine interleukin 15. *Biol Reprod*. 2000;62(4):959–968.
52. Higuma-Myojo S, et al. Cytokine profile of natural killer cells in early human pregnancy. *Am J Reprod Immunol*. 2005;54(1):21–29.
53. King A, Loke YW. Human trophoblast and JEG choriocarcinoma cells are sensitive to lysis by IL-2-stimulated decidual NK cells. *Cell Immunol*. 1990; 129(2):435–448.
54. Lash GE, Robson SC, Bulmer JN. Review: Functional role of uterine natural killer (uNK) cells in human early pregnancy decidua. *Placenta*. 2010; 31(suppl):S87–S92.
55. Kopcow HD, Allan DS, Chen X, et al. Human decidual NK cells form immature activating synapses and are not cytotoxic. *Proc Natl Acad Sci U S A*. 2005; 102(43):15563–15568.
56. Robertson SA, Roberts CT, Farr KL, Dunn AR, Seamark RF. Fertility impairment in granulocyte-macrophage colony-stimulating factor-deficient mice. *Biol Reprod*. 1999;60(2):251–261.
57. Pijnenborg R, Vercruysse L, Hanssens M. The uterine spiral arteries in human pregnancy: facts and controversies. *Placenta*. 2006;27(9–10):939–958.
58. Male V, Gardner L, Moffett A. Isolation of cells from the feto-maternal interface. *Curr Protoc Immunol*. 2012;Chapter 7:Unit 7.40.1-11.
59. Du P, Kibbe WA, Lin SM. lumi: a pipeline for processing Illumina microarray. *Bioinformatics*. 2008; 24(13):1547–1548.
60. Prutsch N, et al. The role of interleukin-1beta in human trophoblast motility. *Placenta*. 2012; 33(9):696–703.